[13] J. Dittmer, A. Nordheim, *Biochim. Biophys. Acta* **1998**, *1377*, F1 – F11.
[14] N. Wernert, *Virchows Arch.* **1997**, *430*, 433 – 443.
[15] N. Wernert, M. B. Raes, P. Lassalle, M. P. Dehouck, B. Gosselin, B. Vandenburger, D. Stehelin, *Am. J. Pathol.* **1992**, *140*, 119 – 127.
[16] N. Wernert, F. Gilles, V. Fafeur, F. Bouali, M. B. Raes, C. Pyke, T. Dupressoir, G. Seitz, B. Vandenburger, D. Stehelin, *Cancer Res.* **1994**, *54*, 5683 – 5688.
[17] C. Iwasaka, K. Tanaka, M. Abe, Y. Sato, *J. Cell Physiol.* **1996**, *169*, 522 – 531.
[18] K. Wakiya, A. Begue, D. Stehelin, M. Shibuya, *J. Biol. Chem.* **1996**, *271*, 30823 – 30828.
[19] R. Crum, S. Szabo, J. Folkman, *Science* **1985**, *230*, 1375 – 1378.
[20] P. Noguiez-Hellin, M. R. Le Meur, J. L. Salzmann, D. Klatzmann, *Proc. Natl. Acad. Sci. USA* **1996**, *93*, 4175 – 4180.
[21] I. Bolon, V. Gouyer, M. Devouassoux, B. Vandenbunder, N. Wernert, D. Moro, C. Brambilla, E. Brambilla, *Am. J. Pathol.* **1995**, *147*, 1298 – 1310.
[22] R. Bicknell, C. E. Lewis, N. Ferrara, *Tumour Angiogenesis*, Oxford University Press, Oxford, **1997**.
[23] D. R. Edwards, G. Murphy, *Nature* **1998**, *394*, 527 – 528.
[24] D. Ingber, T. Fujita, S. Kishimoto, K. Sudo, T. Kanamaru, H. Brehm, J. Folkman, *Nature* **1990**, *348*, 555 – 557.
[25] The p51-Ets-1 protein is the full-length *c-ets-1* transcript, while the p39-Ets-1 protein is a splice-variant lacking the exon VII; see R. J. Fisher, S. Koizumi, A. Kondoh, J. M. Mariano, G. Mavrothalassitis, N. K. Bhat, T. S. Papas, *J. Biol. Chem.* **1992**, *267*, 17957 – 17965.
[26] Treatment of metastatic cervical cancer with TNP-470 in a 49-year-old patient resulted in complete remission, a rare event in this condition: A. P. Kudelka, C. F. Versraegen, E. Loyer, *New Engl. J. Med.* **1998**, *338*, 991 – 992.
[27] a) N. Sin, L. Meng, M. Q. W. Wang, J. J. Wen, W. G. Bornmann, C. M. Crews, *Proc. Natl. Acad. Sci. USA* **1997**, *94*, 6099 – 6103; b) E. C. Griffith, Z. Su, B. E. Turk, S. P. Chen, Y. H. Chang, Z. C. Wu, K. Biemann, J. O. Liu, *Chem. Biol.* **1997**, *4*, 461 – 471; c) E. C. Griffith, Z. Su, S. Niwayama, C. A. Ramsey, Y.-H. Chang, J. O. Liu, *Proc. Natl. Acad. Sci. USA* **1998**, *95*, 15183 – 15188.
[28] S. Liu, J. Widom, C. W. Kemp, C. M. Crews, J. Clardy, *Science* **1998**, *282*, 1324 – 1327.
[29] R. A. Bradshow, W. W. Brickey, K. W. Walker, *Trends Biochem. Sci.* **1998**, *23*, 263 – 267.
[30] J. Taunton, *Chem. Biol.* **1997**, *4*, 493 – 496.
[31] L. F. Fleischman, A. M. Pilaro, K. Murakami, A. Kondoh, R. J. Fischer, T. S. Papas, *Oncogene* **1993**, *8*, 771 – 780.
[32] D. K. Watson, M. J. McWillis, P. Lapis, J. A. Lautenberger, C. W. Schweifest, T. S. Papas, *Proc. Natl. Acad. Sci. USA* **1988**, *85*, 7862 – 7866.
[33] R. K. Jain, K. Schlenger, M. Höckel, F. Yuan, *Nat. Med.* **1997**, *3*, 1203 – 1208.
[34] P. Chomczynski, *Biotechniques* **1993**, *15*, 532 – 534.

A Robust, Environmentally Benign Catalyst for Highly Selective Hydroformylation**

Albertus J. Sandee, Lars A. van der Veen, Joost N. H. Reek, Paul C. J. Kamer, Martin Lutz, Anthony L. Spek, and Piet W. N. M. van Leeuwen*

The hydroformylation of olefins to aldehydes is an important example of an efficient and clean process, because of its potentially 100% atom economy.[1] In the industrial production of C_4 and C_5 aldehydes, where regioselectivity towards the more valuable linear aldehyde product is critical, rhodium – triphenylphosphane complexes are used as catalysts. The products are separated from the catalyst by distillation, which results in catalyst decomposition as an undesirable side reaction. Furthermore, distillation techniques are not suitable for the production of heavier products or fine chemicals because of the high boiling points.

The use of an aqueous biphasic system, in which the water phase contains the dissolved catalyst, affords a straightforward separation of the organic products. To this end, a process using the water-soluble catalyst $[HRhCO(TPPTS)_3]$ (TPPTS = triphenylphosphanyl trisulfonate) has been developed by Ruhrchemie/-Rhône-Poulenc for the hydroformylation of propene.[2] This process meets all the requirements for an environmentally benign process. The applicability of the aqueous biphasic system is, however, strictly limited to substrates that are slightly soluble in water, such as propene and but-1-ene.

A widely investigated approach to facilitate catalyst – product separation is the attachment of the catalyst to a polymeric resin.[3] To date, immobilized catalysts of industrial importance are still unknown: Metal leaching[4] and low catalyst selectivity are the insurmountable problems.

The hydroformylation catalyst that we present here is covalently anchored to a silicate matrix by the sol – gel technique.[5] This material can be prepared by a simultaneous cocondensation of tetraalkoxysilanes and functionalized trialkoxysilanes [Eq. (1)].[6] The sol – gel technique is an ideal method to immobilize catalysts because of its diversity[7] and

$$n\,Si(OR)_4 + 4n\,H_2O \rightarrow n\,Si(OH)_4 + 4n\,ROH \rightarrow \text{polysilicate} \qquad (1)$$

[*] Prof. Dr. P. W. N. M. van Leeuwen, A. J. Sandee, L. A. van der Veen, Dr. J. N. H. Reek, Dr. P. C. J. Kamer
Institute of Molecular Chemistry, Nieuwe Achtergracht 166
1018 WV Amsterdam (The Netherlands)
Fax: (+31) 20-525-6456
E-mail: pwnm@anorg.chem.uva.nl
Dr. M. Lutz, Dr. A. L. Spek
Bijvoet Center for Biomolecular Research
Utrecht (The Netherlands)

[**] We thank Dr. A. Kentgens for performing the solid-state NMR experiments, Dr. J. W. Niemantsverdriet and L. Coulier for help with the XPS measurements, H. Geurts for assistance with the TEM experiments, and J. Elgersma for work with the Rh analyses. We are grateful to the Innovation Oriented Research Program (IOP-katalyse) for the financial support of this research. This work was supported in part (M.L., A.L.S.) by the Council for Chemical Sciences of the Netherlands Organization for Scientific Research (CW-NWO).

Supporting information for this article is available on the WWW under http://www.wiley-vch.de/home/angewandte/ or from the author.

  1433-7851/99/3821-3231 $ 17.50+.50/0

its mildness (recently lipases were successfully immobilized using the sol–gel technique).[8] The few examples, however, of sol–gel-immobilized hydroformylation catalysts reported so far show considerable amounts of metal leaching[9] and low selectivity of the catalyst.[10]

Diphosphanes with a large natural P-M-P bite angle have a beneficial influence on the regioselectivity of homogeneous hydroformylation catalysts.[11] In our group xanthene-based ligands (P-M-P ≈ 110°) were especially designed for this purpose.[12] Overall selectivities of 93% for the linear aldehyde were obtained.[13] A novel xanthene-based ligand, *N*-(3-trimethoxysilane-*n*-propyl)-4,5-bis(diphenylphosphanyl)-phenoxazine (siloxantphos, **A**), was synthesized and immobilized as a rhodium–diphosphane complex in a sol–gel.[14]

On stirring a solution of siloxantphos, $[Rh(acac)(CO)_2]$ (acac = acetylacetonate), and tetramethylorthosilicate (TMOS) in THF/H_2O, the cationic complex $[Rh(siloxantphos)CO]^+$ (**1**, Scheme 1) was formed, which was immobilized in the silica (Figure 1). Interestingly the gelation of these

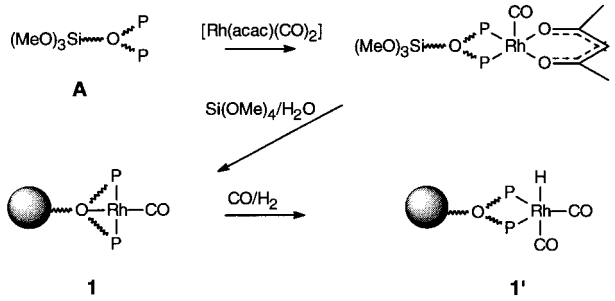

Scheme 1. Schematic illustration of the preparation of sol–gel-immobilized $[HRh(siloxantphos)(CO)_2]$.

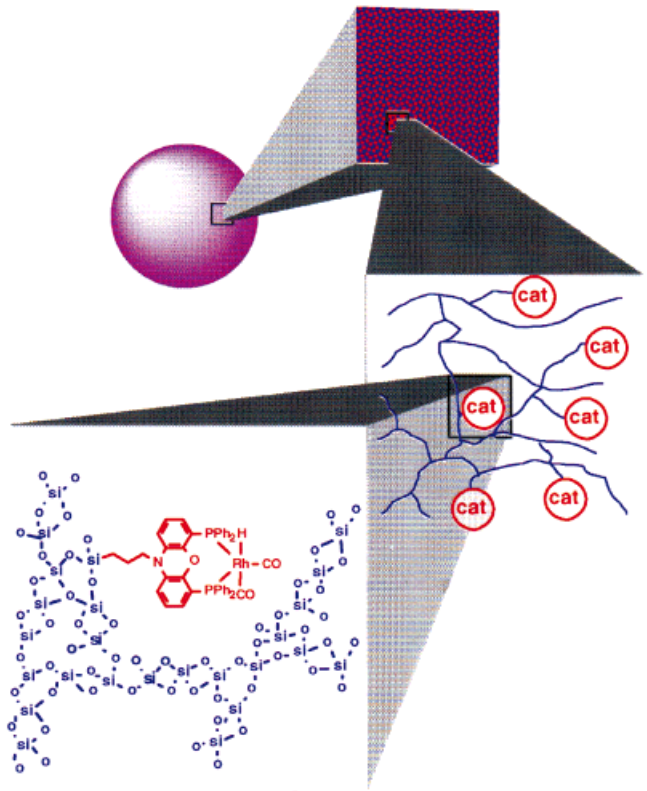

Figure 1. A schematic representation of the sol–gel-immobilized catalyst $[HRh(siloxantphos)(CO)_2]$.

mixtures takes place within one hour without the use of an additive to catalyze the polycondensation of the silica monomers. This suggests that the rhodium–xanthenediphosphane complex acts as a catalyst in this process (the same mixture without **A** has a gelation time of about seven days, even with a large excess of acetylacetone). We observed the formation of the cationic complex by monitoring the sol–gel process of a mixture of 9,9-dimethyl-4,5-bis(diphenylphosphanyl)xanthene (xantphos, **B**) and $[Rh(acac)(CO)_2]$ by

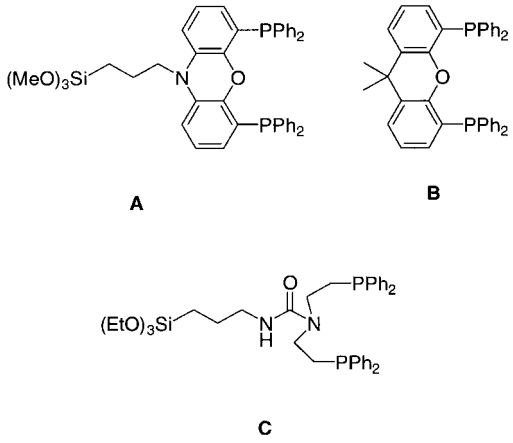

liquid-state ^{31}P NMR spectroscopy. (Nonimmobilized complexes can easily be studied during the sol–gel process by means of liquid-state NMR spectroscopy. This is not possible for the immobilized rhodium–siloxantphos complex.[15]) After [Rh(xantphos)(acac)CO] is formed, this complex quantitatively turns into $[Rh(xantphos)CO]^+$ (**2**) during the gelation process. Probably, acidic silanols, formed during the hydrolysis of TMOS, protonate the acetylacetonate to acetylacetone. As a consequence **2** is formed having a silicate counterion (it cannot be excluded that $acac^-$ is the counterion of these cationic rhodium–diphosphane–carbonyl complexes).

On exposing the gel containing **2** to one atmosphere of CO/H_2 (1/1), the color of the gel changes from orange to yellow. NMR studies showed the transformation from **2** to $[HRh(xantphos)(CO)_2]$ (**2′**), which is the key intermediate for a selective hydroformylation catalyst in a homogeneous phase.[12]

System **1** was characterized by means of solid-state ^{31}P MAS NMR and FT-IR spectroscopy, and both the phosphorus chemical shift and the carbonyl vibration were in good agreement with the fully characterized (homogeneous) complexes **2**(OTf) (Tf = F_3CSO_2) and **2**(BF_4) (Table 1).[16] Using

Table 1. Spectroscopic data for immobilized $[Rh(siloxantphos)CO]^+$ (**1**) and homogenous analogues.[a]

	1	**2**(OTf)	**2**(BF_4)
^{31}P-NMR:			
δ ($J_{P\text{-}Rh}$ [Hz])	38 (br)[b]	36 (br),[b] 37.4 (d, 122)[c]	37.2 (d, 122)[c]
FT-IR:			
$\tilde{\nu}$(CO) [cm^{-1}]	2011	2003	1998

[a] For more details see the Experimental Section. [b] Obtained by means of MAS solid-state NMR spectroscopy; $J_{P\text{-}Rh}$ is too small for detection in the solid state. [c] Obtained by means of liquid-state NMR spectroscopy.

  1433-7851/99/3821-3232 $ 17.50+.50/0

X-ray photoelectron spectroscopy (XPS) we evidenced that rhodium is present purely in the oxidation state I. The binding energies of the rhodium 3d electrons in **1** were found to be 312 and 317 eV with a relative intensity of 3.3 and 2. For **2**(BF_4) similar binding energies of 311 and 316 eV were determined with a relative intensity of 3.2 and 2 (Figure 2). This is in good agreement with the twofold degenerated energy levels of the rhodium 3d electrons known for rhodium(I) compounds.[17] No traces of metallic rhodium(0) were found in the samples.

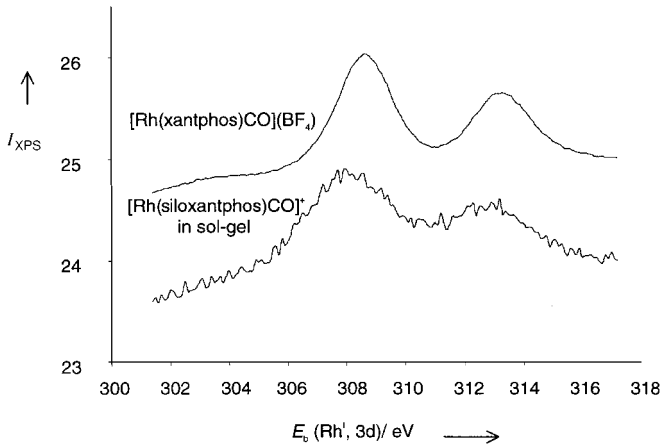

Figure 2. Binding energy of rhodium 3d electrons determined by means of XPS.

The porous nanostructure of the functionalized silica **1** was visualized by means of transmission electron microscopy (TEM) (Figure 3). From the TEM experiments, which were performed without using staining techniques, it was concluded that no clustered rhodium particles were present in the material.[18] This substantiates the results obtained from the XPS experiments.

The crystal structure of **2**(BF_4) shows that in the cationic complex the xanthene ligand coordinates in a tridentate fashion, with the phosphane groups in a *trans* coordination and the ether oxygen atom as a hemilabile donor atom (Rh–O 2.126(3) Å; Figure 4).[19] This POP chelate coordination on rhodium, earlier found for 1,5-bis(diphenylphosphanyl)-3-oxapentane,[20] is likely an important stabilizing factor for the complex during the sol–gel process.[6]

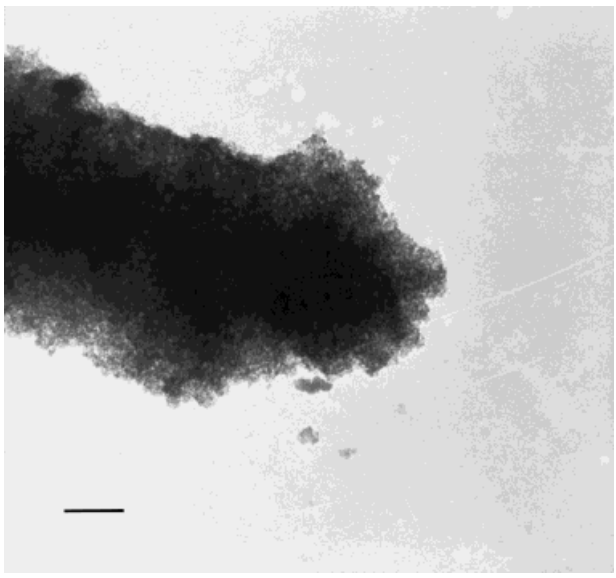

Figure 3. Electron micrograph of an aqueous suspension of sol–gel-immobilized [Rh(siloxantphos)CO]$^+$. The bar represents 100 nm.

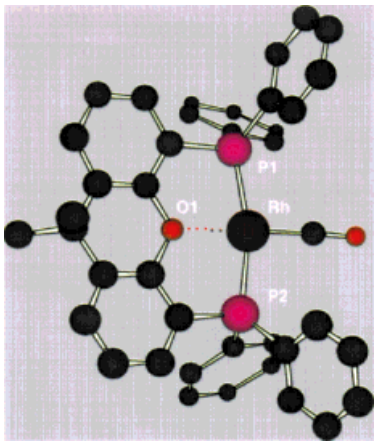

Figure 4. The X-ray structure of [Rh(xantphos)CO](BF_4) (**2**(BF_4)) (hydrogen atoms and the BF_4^- counterion are omitted for clarity). Selected bond distances [Å] and angles [°]: Rh–P1 2.266(11), Rh–P2 2.282(11), Rh–O1 2.126(3), Rh–C(O) 1.798(5); P1-Rh-P2 164.42(4), O1-Rh-C(O) 175.33(19), O1-Rh-P1 83.41(8), O1-Rh-P2 83.68(8).

The catalytic performance of **1** in the hydroformylation of 1-octene was studied in a batch process using 1 g of silica containing 1×10^{-5} mol of rhodium. The selectivity of **1** was as high as 93 % towards the linear aldehyde, which is similar to the value for the homogeneous catalyzed reaction (Table 2, entries 1 and 9). In the absence of the xanthene ligand the selectivity is lowered dramatically (Table 2, entry 8; 26 % *n*-nonanal).

The high selectivity of **1** is induced by the large natural P-Rh-P bite angle. This was proven on comparing **A** (bite angle 108° in **1′**) with a ligand having a much smaller bite angle (93°): *N*-(3-triethoxysilane-*n*-propyl)-*N′*,*N′*-bis[2-(diphenylphosphanyl)ethyl]urea (siloxPNP, **C**).[14, 21] This ligand was sol–gel processed in the same way as **A** (Scheme 1), and immobilized [Rh(siloxPNP)CO]$^+$ (**3**) obtained was subsequently tested in the hydroformylation of 1-octene. The linear-to-branched product ratio using **3** is 15 times lower than for **1** (Table 2, entry 10). This proves that indeed the large P-Rh-P bite angle, as we already reported for the homogeneous systems, plays a key role in the regioselectivity of immobilized systems.

The recyclability of catalyst **1** was studied by performing a series of consecutive runs (Table 2, entries 1–5). We observed no deterioration of the catalytic performance in at least eight cycles. The linear-to-branched ratio remained very high during all experiments and only 2 % of isomers of 1-alkene was formed. The decrease in rate in successive catalytic cycles is very small, indicating that ligand **A** retains the rhodium quantitatively in the solid state. This is confirmed by rhodium analysis on the product by means of atomic emission spectroscopy. No rhodium traces were detected in any of the experiments using **1** and **3**.

  1433-7851/99/3821-3233 $ 17.50+.50/0

Table 2. Results from the hydroformylation of 1-octene at 80 °C and 50 bar CO/H_2.

Entry	Catalyst (cycle)[a]	Conversion [%]	TOF[b]	Linear aldehyde[c] [%]	Branched aldehyde[c] [%]	Alkene isomerization[c] [%]	*n*-Aldehyde hydrogenation[c] [%]	Linear: branched[c]	Rh leaching[d] [%]
1	**1** (1)	69	35	92.8	3.0	1.7	2.5	32:1	< 1
2	**1** (2)	69	36	94.1	2.7	2.0	1.2	36:1	< 1
3	**1** (3)	69	36	94.0	2.7	2.3	1.0	35:1	< 1
4	**1** (4)	67	35	94.5	2.7	2.2	1.3	35:1	< 1
5	**1** (8)	63	33	95.0	2.6	2.0	0.5	37:1	< 1
6	**1**[e]	92	32[f]	95.5	2.3	1.6	0.6	43:1	< 1
7	**1**[g]	63	287	95.5	2.4	1.9	0.3	40:1	< 1
8	$[Rh(acac)(CO)_2]$ in sol-gel[h]	64	175	26.3	16.3	57.4	0.0	1.6:1	> 50
9	**A**/$[Rh(acac)(CO)_2]$ (homogeneous)	19	283	93.3	2.9	3.7	0.0	32:1	–
10	**3**	72	119	70.0	28.9	1.0	0.1	2.4:1	< 1

[a] The ligand-to-rhodium ratio is 10:1; the catalysis was performed in toluene/*n*-propanol (13/1) using 1 mL of 1-octene. [b] Initial turnover frequencies (TOF) were calculated as the amount of aldehyde formed [mol h^{-1}] per mole of catalyst at 10–20% conversion. [c] Determined by means of GC analysis using decane as an internal standard. [d] Determined by means of atomic emission spectroscopy. [e] 3 mL of 1-octene were used. [f] Average turnover frequency. [g] In 14 mL of 1-octene and 1 mL of *n*-propanol. [h] No ligand was used.

Compound **1** is remarkably stable under catalytic conditions. We were able to use the catalyst for more than two weeks without loss of activity and selectivity. Even a three-day run, leaving only a few percent of the substrate unconverted, does not affect the performance of **1** (Table 2, entry 6). This long-term stability indicates that very high turnover numbers can be achieved with this system.

The rate of hydroformylation of 1-octene using **1** has a first-order dependency in substrate concentration, and the exact rate under these specific conditions was determined to be 0.038 [octene].[22] As a consequence we found a high rate of hydroformylation when the reaction was performed in pure octene (initial turnover rate of 287 mol h^{-1} per mol of catalyst; Table 2, entry 7). This rate is about the same as that of the homogeneous catalyzed reaction (283 mol h^{-1} per mol of catalyst) which was performed in toluene (Table 2, entry 9).

Complex **1** is the most selective immobilized hydroformylation catalyst to date. With **1**, the almost ideal situation is reached in that a product, which may have any boiling point or polarity, is isolated in 95% purity after only one simple filtration. Moreover, this system is one of the first examples of a heterogenized catalyst that is free of metal leaching. These features make this novel catalyst perfectly suitable for application in the production of fine chemicals. Furthermore, waste streams are expected to be relatively small because: 1) we find only small amounts of side products, 2) there is no solvent needed, and 3) the catalyst is stable for a long time and shows no metal leaching. It can be concluded that **1** is an interesting environmentally benign catalyst for the selective hydroformylation towards linear aldehydes.

Experimental Section

Synthesis of polysiloxane-bound $[Rh(siloxantphos)CO]^+$: A mixture of $[Rh(acac)(CO)_2]$ (5 mg, 0.01946 mmol) and siloxantphos (138.7 mg, 0.1946 mmol) was dissolved in THF (6 mL). H_2O (2 mL) and TMOS (2 mL) were subsequently added, and a red-brown two-phase system formed. MeOH was added until a clear red-brown solution was formed. Gelation took place within 1 h. After 36 h the gel was carefully dried under reduced pressure. The dried gel was powdered and thoroughly washed with MeOH, THF, and Et_2O. The resulting pink-red silicas were stored at −20 °C. FT-IR (KBr): $\tilde{\nu}$(CO) 2011 cm^{-1}; ^{31}P MAS NMR (121.4 MHz, $NH_4H_2PO_4$ ($\delta = 0.8$)): $\delta = 38$ (br, phosphane), 26 (br, some phosphane oxide), 51 (protonated phosphane).

The recycling experiments were performed as follows. A stainless steel 50-mL autoclave—equipped with a mechanical stirrer, a substrate vessel, a cooling spiral, and a sample outlet—was charged with 1 g of silica, containing 1×10^{-5} mol of rhodium catalyst, in toluene (10 mL) and *n*-propanol (1 mL). The suspension was incubated for 1 h at 80 °C under 20 bar CO/H_2 (1/1). A mixture of 1-octene (1 mL) and decane (1 mL) in toluene (3 mL) was added, and the CO/H_2 pressure was brought to 50 bar. The mixture was stirred for 24 h. The autoclave was cooled down to 10 °C, and the pressure was reduced to 1.8 bar. With the small overpressure the liquid was slowly removed from the catalyst with a 1.2-mm syringe. After the catalyst was washed with toluene (5 mL), toluene (10 mL) was added, and the pressure was brought to 20 bar. Finally the mixture was heated to 80 °C and the second cycle was performed.

Received: June 4, 1999 [Z13513IE]
German version: *Angew. Chem.* **1999**, *111*, 3428–3432

Keywords: hydroformylations · immobilization · rhodium · sol–gel processes

[1] B. M. Trost, *Science* **1991**, *254*, 1471–1477.
[2] E. G. Kuntz, *CHEMTECH* **1987**, 570–575.
[3] F. R. Hartley, *Supported Metal Complexes. A New Generation of Catalysts*, Reidel, Dordrecht, **1985**.
[4] W. A. Herrmann, B. Cornils, *Angew. Chem.* **1997**, *109*, 1074–1095; *Angew. Chem. Int. Ed. Engl.* **1997**, *36*, 1048–1067.
[5] C. M. Ingersoll, F. V. Bright, *CHEMTECH* **1997**, 26–31.
[6] E. Lindner, M. Kemmler, H. A. Mayer, P. Weger, *J. Am. Chem. Soc.* **1994**, *116*, 348–361.
[7] E. Lindner, T. Schneller, F. Auer, P. Weger, H. A. Mayer, *Chem. Eur. J.* **1997**, *3*, 1833–1845.
[8] M. T. Reetz, A. Zonta, J. Simpelkamp, *Angew. Chem.* **1995**, *107*, 373; *Angew. Chem. Int. Ed. Engl.* **1995**, *34*, 301–302.
[9] S. Wieland, P. Panster, *Catal. Org. React.* **1994**, *62*, 383–392.
[10] J. Blum, A. Rosenfeld, N. Polak, O. Israelson, H. Schumann, D. Avnir, *J. Mol. Catal.* **1996**, *107*, 217–223.
[11] C. P. Casey, G. T. Whiteker, M. G. Melville, L. M. Petrovich, J. A. Gavey, D. R. Powell, *J. Am. Chem. Soc.* **1992**, *114*, 5535–5543.
[12] M. Kranenburg, Y. E. M. van der Burgt, P. C. J. Kamer, P. W. N. M. van Leeuwen, K. Goubitz, J. Fraanje, *Organometallics* **1995**, *14*, 3081–3089.
[13] L. A. van der Veen, M. D. K. Boele, F. R. Bregman, P. C. J. Kamer, P. W. N. M. van Leeuwen, K. Goubitz, J. Fraanje, H. Schenk, C. Bo, *J. Am. Chem. Soc.* **1998**, *120*, 11616–11626.

  1433-7851/99/3821-3234 $ 17.50+.50/0

[14] The synthesis of siloxantphos (**A**) and siloxPNP (**C**) will be published elsewhere.
[15] ^{31}P NMR (121.4 MHz, D_2O, H_3PO_4): [Rh(xantphos)(acac)CO]: $\delta = 13$ (d, $J_{P-Rh} = 94$ Hz); $[Rh(xantphos)CO]^+$: $\delta = 37$ (d, $J_{P-Rh} = 121$ Hz).
[16] The stretch frequency of the carbonyl group is slightly influenced by the nature of the counterion of the complexes.
[17] J. W. Niemantsverdriet, *Spectroscopy in Catalysis*, VCH, Weinheim, **1995**.
[18] M. Besson, P. Gallezot, C. Pinel, S. Neto, *Heterog. Catal. Fine Chem. Proc. Int. Symp. IV* **1997**, 215–222.
[19] Crystal structure determination of **2**(BF_4): $C_{40}H_{32}O_2P_2Rh \cdot BF_4 \cdot 0.5\,CH_2Cl_2$, $M_r = 838.78$, yellow needle, $0.75 \times 0.25 \times 0.08$ mm^3, triclinic, space group $P\bar{1}$ (no. 2), $a = 11.5217(10)$, $b = 12.4937(13)$, $c = 13.003(2)$ Å, $\alpha = 91.954(11)$, $\beta = 89.957(11)$, $\gamma = 106.025(8)^\circ$, $V = 1797.9(4)$ Å^3, $Z = 2$, $\rho = 1.549$ g cm^{-3}, $\mu = 0.695$ mm^{-1}. A total of 8558 reflections were measured on an Enraf-Nonius CAD4T diffractometer with rotating anode ($\lambda = 0.71073$ Å) at a temperature of 150(2) K; 8148 reflections were unique ($R_{int} = 0.0483$). The structure was solved with direct methods (SIR97) and refined with SHELXL97 against F^2. R values [$I > 2\sigma(I)$]: $R1 = 0.0538$, $wR2 = 0.1337$. Crystallographic data (excluding structure factors) for the structures reported in this paper have been deposited with the Cambridge Crystallographic Data Centre as supplementary publication no. CCDC-128890. Copies of the data can be obtained free of charge on application to CCDC, 12 Union Road, Cambridge CB2 1EZ, UK (fax: (+44) 1223-336-033; e-mail: deposit@ccdc.cam.ac.uk).
[20] N. W. Alcock, J. M. Brown, J. C. Jeffery, *J. Chem. Soc. Dalton Trans.* **1976**, 583–588.
[21] The bite angles of the ligands were calculated on [Rh(ligand)] as reported in ref. [12].
[22] See the Supporting Information for the determination of the rate equation.

Visualization of Surface Gelation Processes in a Doped Sol–Gel Glass

Germain Puccetti* and Roger M. Leblanc

Sol–gel materials present an alternative to organic polymers and have the advantage of operating at room temperature. This makes them particularly interesting for doping with biological materials.[1, 2] Much work on the chemistry of sol–gel materials aims at adjusting the initial sol composition to control the hydrolysis and condensation reactions according to the desired application of the end material. In situ studies of the evolution of a sol–gel in thin films are based on the optical (for example, fluorescence, interferometry) or mechanical properties (for example, stress) and yield macroscopic information from which the material evolution is inferred.[3–5] Thin-film fabrication is particularly sensitive to the initial chemistry because of the strong influence of environmental constrains over the large exposed surface (air humidity, solvent evaporation).[6–8]

[*] Dr. G. Puccetti, Prof. Dr. R. M. Leblanc
Center for Supramolecular Science and Department of Chemistry
University of Miami
P.O. Box 249118 Coral Gables, FL 33124–0431 (USA)
Fax: (+1) 305-284-1880
E-mail: gpuccett@umiami.ir.miami.edu

The present work reports the first depth-resolved, in situ measurements of the near-surface regions of a material during its evolution from the sol to the gel states. The organic dye molecule β-carotene serves as a probe for the chemical changes that occur during the sol–gel evolution. Depth analysis evidences a clearly distinct chemical evolution at the surface of the material relative to the bulk. This is attributed to the exposition of the surface to air.

Photoacoustic spectroscopy (PAS) relies on optical excitation of a material and measurement of the induced heat release. Despite its simple basic principles, PAS covers a broad range of phenomena that occur during the process of converting absorbed light into the release of heat. Several information factors can be identified that influence, directly or indirectly, the energy conversion process: a) the light absorption coefficient; b) the molecular-level de-excitation process; c) the excitation/heat transfer to the molecular environment; d) heat propagation; and e) the spatial distribution of microscopic heat sources inside the sample. The characterization of any material by PAS is governed by three main material properties: 1) the light absorption distribution (Beer's law); 2) the thermal diffusion; and 3) the thickness of the material being investigated.[9, 10]

The relative importance of the aforementioned information factors can be modified by choosing sample conditions so as to eliminate some of them.[11] In the present study, thin samples and a low dopant concentration allow us to neglect three out of the five factors. Two dominant information factors influence the response signal: energy transfer from β-carotene to its microscopic environment (c) and variable thermal properties of the sample (d). However, a previous study has shown that the changes in the thermal property of the sample (during the sol to gel evolution) are small with respect to the energy transfer factor.[11] The measured signal is therefore dominated by changes in the efficiency of heat transfer from β-carotene molecules to their immediate molecular environment. This dopant molecule was chosen because of its very good stability in sol–gel materials and its near unit thermal de-excitation conversion yield.[12–14]

A thicker sample (about 1 mm) was used initially to simulate bulk sol–gel material during its chemical aging. The depth-dependent heat emission that was extracted from the time response signal, obtained from pulsed photoacoustic spectroscopy (PPAS), versus time of aging is given in Figure 1b. The classical PPAS signal (Δp_{max}, t_{max}) is added for comparison (Figure 1a). Studies of the dopant dynamics of a tetramethoxysilane (TMOS)/dimethylaminopyridine (DMAP) sol–gel have shown that the sol phase is characterized by an increase in length of polymers with time which results in an increasing viscosity of the medium.[15] Macroscopic gelation occurs when the longer polymer species are consumed to form the long-distance network. This process results in a temporary decrease in hindrance (local viscosity) around dopant molecules and β-carotene experiences a sudden return to a solventlike environment.

The depth-resolved signal (Figure 1b) reveals two distinct time evolutions: near the sample surface (less than 11 μm) and in its bulk (greater than 11 μm). These were not apparent on the global response signal (Figure 1a) as obtained by classical

  1433-7851/99/3821-3235 $ 17.50+.50/0